

# Non-thermal properties of SNR G1.9+0.3

L.T. Ksenofontov\*, H.J. Völk<sup>†</sup>, E.G. Berezhko\* and V.K. Yelshin\*

\*Yu.G. Shafer Institute of Cosmophysical Research and Aeronomy, 31 Lenin Ave., 677980 Yakutsk, Russia

<sup>†</sup>Max Planck Institut für Kernphysik, Postfach 103980, D-69029 Heidelberg, Germany

**Abstract.** Nonlinear kinetic theory of cosmic rays acceleration in supernova remnants (SNRs) is used to investigate the properties of the presumably youngest Galactic SNR G1.9+0.3. The observed angular size and expansion speed as well as the radio and X-ray emission measurements are used to determine the relevant physical parameters of this SNR. Under the assumption that SNR G1.9+0.3 is near the Galactic center (at the distance  $d = 8.5$  kpc) we calculated all relevant SNR properties. In particular, the expected TeV-gamma ray energy flux is as low as  $F \approx 2 \times 10^{-15}$  erg/(cm<sup>2</sup>s), strongly dependent upon the source distance  $F \propto d^{-11}$ .

**Keywords:** acceleration of particles — X-rays: individual (G1.9+0.3) — gamma rays: observations

## I. INTRODUCTION

G1.9+0.3 has been known as a potential young shell type Galactic supernova remnant (SNR) of smallest angular size [1]. Recently, the interest in this SNR was revived by [2] who analyzed the expansion of this SNR and deduced an age  $t_{SN}$  of about 100 years, making it the youngest known SNR in the Galaxy. Although the expansion rate is derived comparing radio observations in 1985 and *Chandra* observations in 2007, it has been immediately confirmed by independent radio observations [3], [4].

The linefree X-ray emission has a pure synchrotron origin [2] which clearly indicates that effective acceleration of CRs takes place at least for electrons.

There are some arguments, like the bilateral symmetry of the X-ray synchrotron emission suggesting a roughly uniform ambient magnetic field, that favor a type Ia origin for G1.9+0.3 [2].

The distance estimate  $d = 8.5$  kpc is based on an analysis of the absorption towards G1.9+0.3 [2].

During the survey of the inner Galaxy by H.E.S.S. in very-high energy  $\gamma$ -rays no emission was reported from the direction to G1.9+0.3 [5]. Therefore one can derive a minimum upper limit at the level of 2% of the Crab flux above 200 GeV.

In this paper time-dependent kinetic theory of cosmic rays acceleration in SNRs [6], [7] is applied, in order to study the nonthermal properties of G1.9+0.3.

## II. MODEL

Following [2] it is assumed that G1.9+0.3 is a type Ia supernova which therefore presumably expands into a uniform interstellar medium (ISM), ejecting roughly

a Chandrasekhar mass  $M_{ej} = 1.4M_{\odot}$ . During an initial period the ejecta material has a broad distribution in velocity  $v$ . The fastest part of these ejecta is described by a power law  $dM_{ej}/dv \propto v^{2-k}$  with  $k = 7$  [8].

The ISM gas density  $\rho_0 = 1.4m_p N_H$ , which is usually characterized by the hydrogen number density  $N_H$ , is an important parameter which strongly influences the expected SNR dynamics and nonthermal emission. Here  $m_p$  is the proton mass.

The value of the SN explosion energy  $E_{sn} = 10^{51}$  erg is taken as typical for type Ia SNe.

The observed shock size  $R_s = 2$  kpc and the shock speed  $V_s = 14000$  km/s are used to determine for a given source distance  $d$  the SNR age  $t_{SN}$  and the ISM number density  $N_H$ .

Following [2] the distance  $d = 8.5$  kpc is adopted.

Nonlinear kinetic theory of CR acceleration in SNRs [6], [7] is applied, in order to find the optimum set of physical parameters of G1.9+0.3, which give a consistent description of the observed overall dynamics and of the nonthermal emission.

The theory includes all the important physical factors which influence CR acceleration and SNR dynamics: shock modification by CR backreaction, MHD wave damping within the shock transition, a consistently determined CR spectrum, and the spatial distributions in each evolutionary phase. In addition it includes synchrotron losses of CR electrons and a determination of all non-thermal emission processes, produced in SNRs by the accelerated CRs. It had also been shown that the values of these key parameters (proton injection rate  $\eta$ , electron to proton ratio  $K_{ep}$  and upstream magnetic field strength  $B_0$ ) which can not be predicted theoretically with the required accuracy, can be determined from a fit of the observed synchrotron emission data [9], [10].

Since in all young SNRs magnetic field is considerably amplified so that some essential fraction of the shock energy  $\rho_0 V_s^2$  is converted into magnetic field energy [10], we use here the time dependent magnetic field strength

$$B_0(t) = B_0(t_{SN})V_s(t)/V_s(t_{SN}). \quad (1)$$

The X-ray morphology agrees with the theoretical expectations regarding the morphology of ion injection and the corresponding morphology of magnetic field amplification [11]. It is therefore consistent with a correction for the spherically symmetric solution by a renormalization factor  $f_{re} \approx 0.2$ .

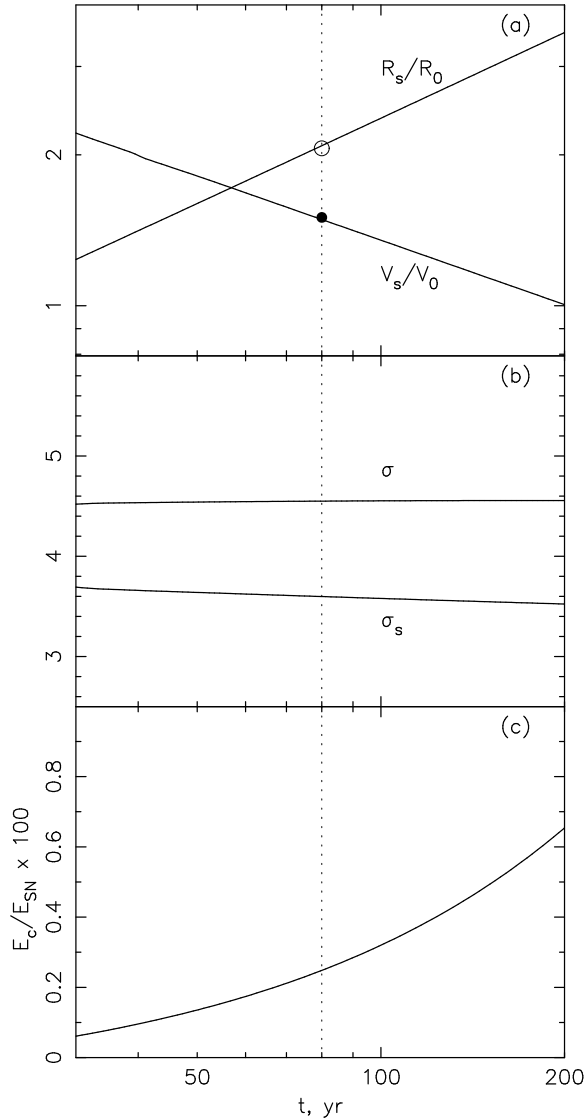


Fig. 1. Shock radius  $R_s$  and shock speed  $V_s$  in units of  $R_0 = 2$  pc and  $V_0 = 10^4$  km/s (a), total shock  $\sigma$  and thermal subshock  $\sigma_s$  compression ratios (b) and total energy content of accelerated CRs  $E_c$  (c) as functions of time. The dotted vertical line marks the current epoch,  $t_{SN} = 80$  yrs. The observed mean size (open circle) and speed (filled circle) of the shock, as determined by X-ray measurements [2], are shown as well.

### III. RESULTS

The calculated evolution of the dynamical parameters of G1.9+0.3 is shown in Fig.1. The observed shock radius and shock speed are fitted at the age  $t_{SN} = 80$  yrs and at the ISM hydrogen number density  $N_H = 0.015$  cm $^{-3}$  (Fig.1a). Since the remnant is in a free-expansion phase, it is consistent with an analytical self-similar solution [8]. Note, that the model of explosion with an exponential ejecta velocity profile gives slightly larger values of the age  $t_{SN} = 100$  yrs and of the ISM number density  $N_H \approx 0.03$  cm $^{-3}$  for the same assumed distance  $d = 8.5$  kpc [2].

To obtain a good fit for the observed synchrotron spectrum (see below) we assume a proton injection rate  $\eta = 10^{-3}$ . It leads to a significant nonlinear modification

of the shock which, at the current age of  $t = 80$  yrs, has a total compression ratio  $\sigma = 4.7$  and a subshock compression ratio  $\sigma_s = 3.6$  (Fig.1b).

With the renormalization the CRs inside G1.9+0.3 SNR contain (Fig.1c)

$$E_c = 0.003 f_{re} E_{SN} \approx 6 \times 10^{47} \text{ erg.} \quad (2)$$

The volume-integrated (or overall) CR spectrum

$$N(p, t) = 16\pi^2 p^2 \int_0^\infty dr r^2 f(r, p, t) \quad (3)$$

has, for the case of protons, almost a pure power-law form  $N \propto p^{-\gamma}$  over a wide momentum range from  $0.1 m_p c$  up to the cutoff momentum  $p_{max} \approx 3 \times 10^6 m_p c$  (Fig.2). This value  $p_{max}$  is limited mainly by the finite size and speed of the shock, its deceleration and the adiabatic cooling effect in the downstream region [12]. G1.9+0.3 then represents the youngest SNR where the accelerated proton spectrum extends up the so-called knee energy, that is indeed needed to describe the overall CR spectrum at energies up to  $10^{17}$  eV [13].

The shape of the overall electron spectrum  $N_e(p)$  deviates from that of the proton spectrum  $N(p)$  at high momenta  $p > p_1 \sim 10^3 m_p c$ , on account of the synchrotron losses during their residence time in the downstream region. Within the momentum range  $p_1 < p < p_{max}^e$ , the electron spectrum is considerably steeper  $N_e \propto p^{-3}$  due to synchrotron losses taking place in the downstream region after the acceleration at the shock front. The maximum electron momentum  $p_{max}^e \approx \times 10^5 m_p c$  is the result of equating the synchrotron loss time and the acceleration time.

Fig. 2 illustrates the consistency of the synchrotron spectrum, calculated at the best set of injection parameters – proton injection rate  $\eta = 10^{-3}$  and electron to proton ratio  $K_{ep} = 3 \times 10^{-4}$  – with the observed spatially integrated spectra. The required upstream magnetic field strength at the current epoch is  $B_0(t_{SN}) = 89.4 \mu\text{G}$ . It gives a downstream magnetic field strength  $B_d = 420 \mu\text{G}$ .

Values  $\alpha > 0.5$  of the radio spectral index  $\alpha = -d \ln S_\nu / d \ln \nu$ , as observed in young SNRs, require a curved electron spectrum that hardens to higher energies as predicted by nonlinear shock acceleration models. To have  $\alpha = 0.62$  in the radio range, as observed for G1.9+0.3 [3], one needs efficient CR acceleration with a proton injection rate  $\eta = 10^{-3}$  which leads to the required shock modification, and also leads to the high interior magnetic field  $B_d = 420 \mu\text{G}$ . Such a high downstream magnetic field, leading to the strong synchrotron cooling of X-ray emitting electrons, is also required to fit Chandra X-ray data (Fig.2). The hard power law X-ray spectrum continues almost up to 50 keV making this source attractive to observe with the Suzaku and INTEGRAL X-ray missions.

For comparison, through the dotted curve, a synchrotron spectrum is included, which corresponds to an artificial leptonic scenario with a proton injection rate

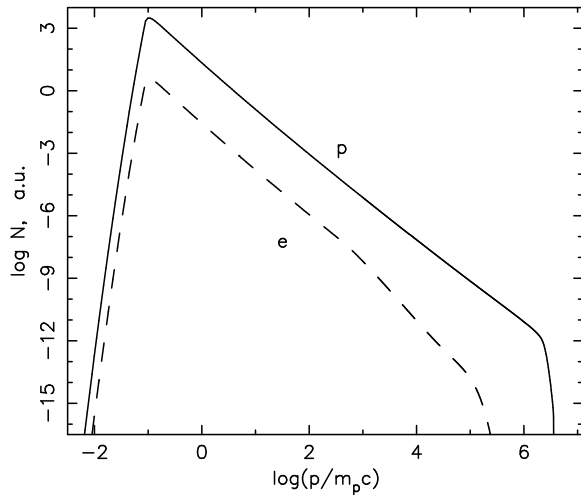


Fig. 2. Spatially integrated CR spectrum as function of particle momentum. *Solid and dashed lines* correspond to protons and electrons, respectively.

so small ( $\eta \ll 10^{-4}$ ) that the accelerated nuclear CRs do not produce any significant shock modification and therefore also no magnetic field amplification. This corresponds to the test particle limit, when the distribution function of shock accelerated electrons has the form

$$f_e \propto p^{-4} \exp(-p/p_{\max}). \quad (4)$$

Since magnetic field amplification is not expected in this case, the downstream magnetic field can not be larger than compressed ISM field  $B_{\text{ISM}} = 5 \mu\text{G}$ . The maximal possible field  $B_d = 20 \mu\text{G}$  is adopted, which corresponds to the minimal number of accelerating electrons and therefore the  $\gamma$ -ray emission, produced by these electrons, is also minimal. The synchrotron spectrum for the leptonic scenario in Fig.3 corresponds to the maximal electron energy  $\epsilon_{\max} = p_{\max}c = 6 \text{ TeV}$ . There are two differences in the synchrotron spectra, corresponding to these two scenarios. The high-injection scenario leads to a steep radio spectrum  $S_\nu \propto \nu^{-\alpha}$  with power law index  $\alpha = 0.62$  whereas in the test particle case  $\alpha = 0.5$ . On the other hand the two spectra behave essentially different at X-ray frequencies  $\nu \gtrsim 10^{18}$ . They demonstrate that only in the high-injection case with its high, amplified magnetic field value  $B_d \approx 400 \mu\text{G}$  the spectrum  $S_\nu(\nu)$  has a smooth cutoff consistent with the experiment (see Fig.3). In the test particle case the spectrum  $S_\nu(\nu)$  has too sharp a cutoff to be consistent with the observations.

In Fig.4 the calculated  $\gamma$ -ray energy fluxes due to  $\pi^0$ -decay and inverse Compton (IC) are presented together with the sensitivities of the Fermi and H.E.S.S. instruments. The expected TeV  $\gamma$ -ray energy flux is about  $\epsilon_\gamma F_\gamma \approx 2 \times 10^{-15} \text{ erg}/(\text{cm}^2\text{s})$  which is too low for a potential detection.

It is however noted that the expected  $\gamma$ -ray flux is very sensitive to the source distance. Therefore the remnant G1.9+0.3 could be a potential  $\gamma$ -ray source if the actual

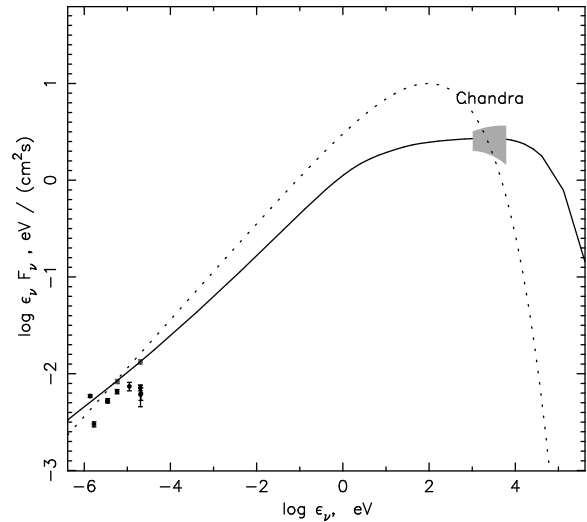


Fig. 3. Synchrotron energy flux as a function of frequency. Fluxes of the X-ray emission observed by *Chandra* [2] and the radio emission compiled by [3] are also shown. Lines are fitted to the most recent VLA radio data reported by [3].

distance was lower than 8.5 kpc. Qualitatively, the dependence of the expected  $\gamma$ -ray flux on the distance can be understood if one takes into account that distance  $d$  and ISM density  $N_{\text{H}}$  are connected by the relation

$$N_{\text{H}} \propto d^{-7}, \quad (5)$$

because in the free expansion phase the SNR radius  $R_s \propto d$  is determined by the expression  $R_s \propto N_{\text{H}}^{-1/7} t^{4/7}$ . Taking into account the dependence of the  $\pi^0$ -decay  $\gamma$ -ray flux on the relevant parameters

$$F_\gamma \propto N_{\text{H}}^2 V_s^2 R_s^3 / d^2, \quad (6)$$

together with the fact that  $V_s \propto d$ , we have

$$F_\gamma \propto d^{-11}. \quad (7)$$

According to this relation a mere 30% reduction of the source distance leads to an increase of the expected  $\gamma$ -ray flux by a factor of about 100. This is illustrated in Fig.4, where we present also  $\gamma$ -ray spectra, calculated for the distance value  $d = 5.6 \text{ kpc}$ . It is clear that G1.9+0.3 could be visible in TeV  $\gamma$ -rays by present instruments, like H.E.S.S., if the actual distance was not larger than  $d = 5.6 \text{ kpc}$ .

As it is seen from Fig.4, the TeV  $\gamma$ -ray flux expected in the leptonic scenario considerably exceeds the H.E.S.S. sensitivity, corresponding to  $\sim 100 \text{ h}$  observational time. Since the region of the Galactic center was already explored by H.E.S.S. for times of about 100 h without detection of G1.9+0.3, the leptonic scenario should be rejected as in all similar cases.

The calculated radio synchrotron flux increases with time, as can be seen in Fig.5, mainly due to the rapidly increasing total number of accelerated electrons. This is in consistent with observations.

At the same time, the X-ray synchrotron flux is expected to be nearly constant in time. This is mainly

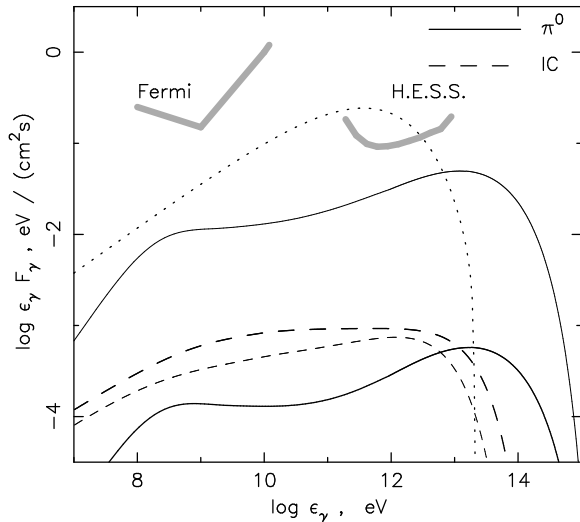


Fig. 4. Integral  $\pi^0$ -decay (solid lines) and IC (dashed lines)  $\gamma$ -ray energy fluxes as a function of  $\gamma$ -ray energy for the two different source distances  $d = 8.5$  kpc (thick lines) and  $d = 5.6$  kpc (thin lines). The dotted spectrum corresponds to a purely leptonic scenario (see text). For comparison, the sensitivities of *Fermi* (1 year observation) [14] and H.E.S.S. [15] are shown.

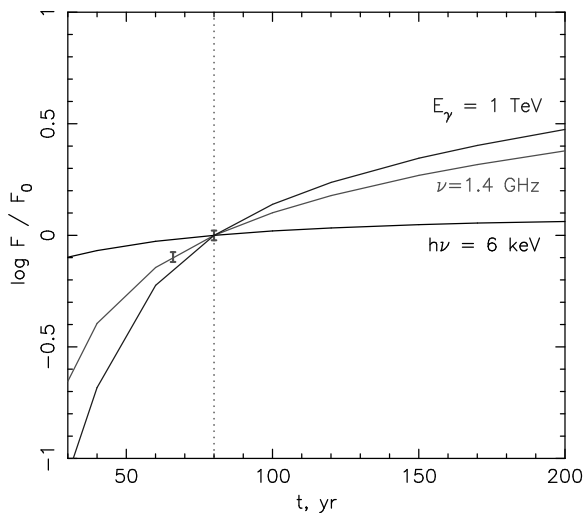


Fig. 5. Lightcurves in nonthermal radio, X-rays and  $\gamma$ -rays for the source distance  $d = 8.5$  kpc, normalized to the current flux. The available radio data [3] are also shown.

due to strong synchrotron cooling of the highest-energy electrons which produce the X-ray synchrotron emission.

The TeV  $\gamma$ -ray flux is expected to increase with time (Fig.5), mainly due to the increase of overall number of CRs with energy about 10 TeV.

#### IV. CONCLUSIONS

The existing data for G1.9+0.3, analyzed within the nonlinear kinetic theory of CR production in SNRs, are consistent with a type Ia explosion at a distance of  $d = 8.5$  kpc. Unfortunately this data set is not complete enough to determine the values of relevant physical parameters, in particular the value of the source distance. Since the expected  $\gamma$ -ray flux is very sensitive to the distance value  $F_\gamma \propto d^{-11}$ , measurements of the  $\gamma$ -ray flux from G1.9+0.3 would give information about the distance. However, in the case when G1.9+0.3 is situated near the Galactic center ( $d = 8.5$  kpc) the expected TeV  $\gamma$ -ray emission is so low,  $\epsilon_\gamma F_\gamma \approx 2 \times 10^{-15}$  erg/(cm<sup>2</sup>s), that it can not be measured by the present instruments. Only if the actual distance was not larger than 5.6 kpc, then G1.9+0.3 could be visible in high energy  $\gamma$ -rays .

#### V. ACKNOWLEDGMENTS

We are indebted to Dr. Stephen Reynolds for providing us the X-ray spectra for G1.9+0.3 from Chandra in physical units. This work has been supported in part by the Russian Foundation for Basic Research (grant 07-02-00221), Programm of PRAS No. 16 and by the Leading Scientific Schools of Russia (project 3968.2008.2). EGB and LTK acknowledge the hospitality of the Max-Planck-Institut für Kernphysik, where part of this work was carried out.

#### REFERENCES

- [1] Green, D.A., & Gull, S.F. 1984, *Nature*, 312, 527
- [2] Reynolds, S.P., et al. 2008, *ApJ*, 680, L41
- [3] Green, D.A., et al. 2008, *MNRAS*, 387, L54
- [4] Murphy, T., Gaensler, B.M., & Chatterjee, S. 2008, *MNRAS*, 389, L23
- [5] Aharonian, F., et al. 2006, *ApJ*, 636, 777
- [6] Berezhko, E.G., Elshin, V.K., & Ksenofontov, L.T. 1996, *J. Exp. Theor. Phys.*, 82, 1
- [7] Berezhko, E.G., & Völk, H.J. 1997, *Astroparticle Phys.*, 7, 183
- [8] Chevalier, R.A. 1982, *ApJ*, 258, 790
- [9] Berezhko, E.G. 2005, *Adv. Space Res.*, 35, 1031
- [10] Berezhko, E.G. 2008, *Adv. Space Res.*, 41, 429
- [11] Völk, H. J., Berezhko, E. G., & Ksenofontov, L. T. 2003, *A&A*, 409, 563
- [12] Berezhko, E.G. 1996, *Astropart. Phys.*, 5, 367
- [13] Berezhko, E.G. & Völk, H.J. 2007, *ApJ*, 661, L175
- [14] Weekes, T. C. 2003, in *Proc. 28th ICRC (Tsukuba)*, eds. T. Kajita, Y. Asaoka, A. Kawachi, Y. Matsubara, & M. Sasaki (Tokyo, Japan: Universal Academy Press Inc.), 8, 3
- [15] Funk, S. 2005, in *Ph.D. Thesis*, Univ. of Heidelberg, Germany, 71